JMEPEG (2007) 16:224–228
DOI: 10.1007/s11665-007-9036-0

1059-9495/$19.00

A New Methodology for Ductile Fracture Criteria to Predict the Forming Limits

Fahrettin Ozturk and Daeyong Lee

(Submitted July 21, 2006)

The main objective of this study was to develop an improved method for an application of ductile fracture criteria to predict forming limit diagram (FLD) of the sheet metals. Neck initiation was studied experimentally and numerically for a tensile test. Based on the results, a new methodology regarding the ductile fracture criteria was proposed to estimate forming limits. The new methodology states that the fracture criteria constant could be calculated at a thickness strain in the range of 20–25%, and be considered as a critical value of the ductile fracture criteria for strain localization. The new proposed methodology was successful in predicting the left side of the FLD and more refinement is needed to predict the right side of the FLD.

Keywords ABAQUS, ductile fracture criteria, formability, forming limit diagram, out-of-plane strain

1. Introduction

Forming limit diagram (FLD) has been commonly used to evaluate the formability of sheet metals for diagnosing the possible production problems in sheet metal stamping. It indicates the limit strains corresponding to the onset of localized necking over a range of major-to-minor strain ratios. The FLD is usually determined by localized necking. However, necking prediction is a complex process and is not easily determined. Experimental procedures require tremendous amount of effort and special equipments. It also depends on the accuracy of the equipment and the experience of the experimenter. Moreover, there has not been any well-accepted analytical and numerical procedure available to predict the FLD.

Recently, several researchers (Ref 1–4) have used ductile fracture criteria *to* determine the limit strains. The limit strains *were* determined by substituting the values of stress and strain histories calculated by the finite element simulations into the ductile fracture criteria. There are some successful predictions for the fracture process, but no full determination of the FLD was successfully constructed by such efforts.

The energy or generalized plastic work criterion was first given by Freudenthal (Ref 5)

$$\int_0^{\bar{\varepsilon}_f} \bar{\sigma} d\bar{\varepsilon} = C \qquad \text{(Eq 1)}$$

Fahrettin Ozturk, Department of Mechanical Engineering, Nigde University, Nigde 51100, Turkey; and **Daeyong Lee,** Department of Mechanical Engineering, Rensselaer Polytechnic Institute, Troy, NY 12180. Contact e-mail: fahrettin@nigde.edu.tr.

where $\bar{\sigma}$ and $\bar{\varepsilon}$ are the equivalent (Mises) stress and strain, respectively. C is the critical value for fracture.

Cockcroft and Latham (Ref 6) proposed a fracture criterion based on "true ductility," which states that the fracture in a ductile material occurs when the following condition is satisfied:

$$\int_0^{\bar{\varepsilon}_f} \bar{\sigma}\left(\frac{\sigma^*}{\bar{\sigma}}\right) d\bar{\varepsilon} = C \qquad \text{(Eq 2)}$$

where $\bar{\sigma}$ is the equivalent stress, $\bar{\varepsilon}_f$ is the fracture strain, $\bar{\varepsilon}$ is the equivalent strain, σ^* is the highest tensile stress, and $\frac{\sigma^*}{\bar{\sigma}}$ is non-dimensional stress-concentration factor, which represents the effect of the highest tensile stress. The reduced form of the Cockcroft and Latham criterion is as follows:

$$\int_0^{\bar{\varepsilon}_f} \sigma^* d\bar{\varepsilon} = C \qquad \text{(Eq 3)}$$

Here, σ^* is calculated using the equation of Bridgman (Ref 7).

The Cockcroft and Latham criterion was modified by Brozzo et al. (Ref 8) to introduce the effect of hydrostatic stress σ_h in an explicit form and to correlate their experimental results.

$$\int_0^{\bar{\varepsilon}_f} \frac{2\sigma^*}{3(\sigma^* - \sigma_h)} d\bar{\varepsilon} = C. \qquad \text{(Eq 4)}$$

Oh et al. (Ref 9) modified the Cockcroft and Latham criterion as follows:

$$\int_0^{\bar{\varepsilon}_f} \left(\frac{\sigma^*}{\bar{\sigma}}\right) d\bar{\varepsilon} = C. \qquad \text{(Eq 5)}$$

Norris et al. (Ref 10) proposed a fracture criterion based on plastic strain. The form of the fracture criterion is given by

$$C = \int f(\sigma_h) d\bar{\varepsilon}^p \text{ or } C = \int_0^{\bar{\varepsilon}_f} \frac{d\bar{\varepsilon}}{1 - c\sigma_h} \quad \text{(Eq 6)}$$

where c is approximately calculated by

$$c = \frac{1}{3.1\text{YS}} \quad \text{(Eq 7)}$$

where YS is the yield stress of the material. Atkins (Ref 11) modified the Norris et al. (Ref 10) criterion to accommodate sheet metal behavior as follows:

$$C = \int_0^{\bar{\varepsilon}_f} \frac{(1 + \frac{1}{2L})}{1 - c\sigma_h} d\bar{\varepsilon} \quad \text{(Eq 8)}$$

where $L = \frac{d\varepsilon_1}{d\varepsilon_2}$ is the strain ratio of in-plane strains.

Ozturk and Lee (Ref 12) successfully determined the fracture strains by the generalized plastic work (Ref 5), Cockcroft and Latham (Ref 6), and Oh et al. (Ref 9) criteria for the left side of the FLD ($\varepsilon_1 \geq 0$, $\varepsilon_2 \leq 0$). Brozzo et al. (Ref 8), Norris et al. (Ref 10), and Atkins (Ref 11) criteria also determined the fracture strain successfully, but slightly higher than the experimental values. The predictions at the right side of the FLD ($\varepsilon_1 \geq 0$, $\varepsilon_2 \geq 0$) for Hill's model were not acceptable, because the predicted data are much lower than the experimental and analytical FLDs. The Mises model fracture predictions at the right side of the FLD were more reasonable than the Hill model. The Mises model seems to show a better agreement but underpredicts the necking.

All of these criteria could not be directly used to determine the FLD of sheet metal alone. It is needed to investigate an improved method for an application of ductile fracture criteria to predict FLD of the sheet metals. In this study, neck initiation during tensile test was studied both experimentally and numerically. Based on the results, a new methodology was proposed to estimate the ductile fracture criteria for the strain localization process. The fracture criteria constants were calculated using the tensile test simulation data for 20 and 25% thickness strain. Then FLDs were constructed using the modified methodology to the ductile fracture criteria and the results were compared against the experimental and analytical results.

2. Experimental Set Up and Mechanical Measurements

The material used in this study was aluminum killed drawing quality electrogalvanized (AKDQ) steel. The coating weight was 70G/70G, which meant that there was a minimum of 70 g of zinc present on each m^2 of sheet metal. The compositions of AKDQ steel are given in Table 1.

Table 1 Chemical composition of the AKDQ steel, wt.%

C	Mn	P	S	Si	Cr	Ni	Mo
0.0378	0.18	0.008	0.0043	0.003	0.012	0.006	< 0.003
Cu	Al	Ti	Cb	V	B	Ca	N
0.018	0.053	< 0.003	< 0.003	< 0.003	< 0.0003	< 0.0003	0.0110

Tensile tests were performed to determine the mechanical properties. An Instron screw-driven type test machine was used to perform the testings. Two extensometers were used to measure longitudinal and width strains. The measured mechanical properties of the AKDQ steel are summarized in Table 2. For example, Young's modulus of this steel is 200 GPa at 20 °C. As shown in Table 2, manufacturer anisotropy data are slightly different than the measured values. The anisotropy data suggested by the supplier were used in the simulation work due to the difficulty of attaching the width extensometer to the specimen during the testing. True stress vs. true strain curve was determined for each direction based on average of several tensile test data (Fig. 1). True stress vs. true strain curve was converted to true stress vs. true plastic strain curve in order to define mechanical properties data in ABAQUS/Standard for the simulation of the tensile test. In tensile test, after reaching the maximum load, thickness and width strains were manually measured. These measurements were achieved by loading the material, taking the measurements, and unloading. This process was repeated at least five times. At each step, width and thickness were measured. This process was done for the specimens of rolling (0°) and transverse (90°) directions.

3. Finite Element Simulation

The tensile test was simulated using finite elements to see neck initiation and to calculate the ductile fracture criteria constant accurately. Only a quarter of the tensile test specimen as shown in Fig. 2 was modeled, due to the symmetry of geometry, using MSC PATRAN. The problem was treated as a plane stress problem due to the thin thickness of the specimen. Continuum plane stress four node reduced integration element (CPS4R) was used. Since the elements have one integration point, they should be used with reasonably fine meshes to prevent locking (Ref 13). Symmetry boundary conditions on the faces, XSYMM (degrees of freedom 1, 5, 6 = 0) and YSYMM (degrees of freedom 2, 4, 6 = 0) were applied. Finite element meshing of this specimen geometry is shown in Fig. 3. Mesh sensitivity study was also performed to find optimum mesh size.

Table 2 Summary of material properties of the AKDQ steel

Tensile direction	Yield strength, MPa (0.2%)	Ultimate tensile strength, MPa	Total elongation, 50 mm %	True fracture strain ε_f^{true}, %	Anisotropy, r	Strength coefficient, MPa	Strain hardening coefficient, n
0°	170	290	49.6	74	1.83(1.58[a])	482.27	0.215
45°	182	295	38.6	66	1.28(1.35[a])	493.09	0.191
90°	170	280	46.4	73	2.60(2.20[a])	465.94	0.200
Ave.	174	288.33	44.87	71	1.75	480.43	0.202

[a]Manufacturer data

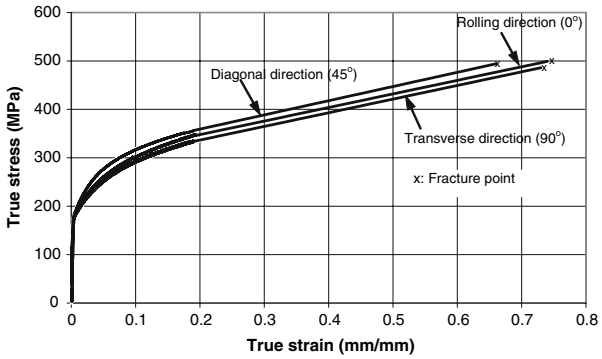

Fig. 1 True stress vs. true strain curves for the AKDQ steel

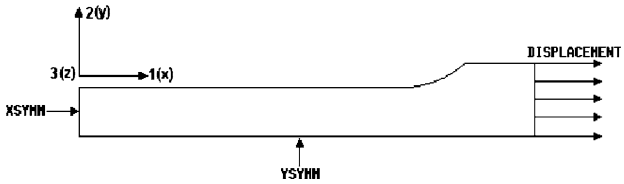

Fig. 2 Geometric modeling of tensile test

Fig. 3 Finite element meshing of tensile specimen

Fig. 4 Deformed meshes of tensile specimen

In the simulation, Hill's yield potential was used in ABAQUS/Standard to model anisotropic plasticity. In addition, the problem was analyzed by Mises' yield criterion. The reason is that Hill's criterion overestimates the effect of the *R*-value on shape of the yield loci (Ref 14, 15). Finally, displacement boundary condition were applied and problem was solved by both Hill's and Mises' models. Stress and strain histories were recorded. The deformed tensile test based on numerical simulation sample is shown in Fig. 4.

Forming limit diagram was experimentally determined for the AKDQ steel by out-of-plane test method to make a comparison between experimental and numerical results. The details of this work is given in (Ref 16). Analytical FLD was determined based on well-established instability criteria. The left side of the FLD was predicted by Hill criterion for localized necking in thin sheets under plane stress condition (Ref 17). The right side of the FLD was determined by Swift's diffuse necking equation (Ref 18). The effect of thickness (Ref 19) was also included to determine the analytical FLD. Details of numerical method were well-defined by of Ozturk and Lee (Ref 12). The FLDs were predicted by various ductile fracture criteria with this new proposed methodology.

4. Results and Discussion

Tensile test was used to investigate the neck initiation. In the experimental results, Fig. 5 clearly indicates that localized necking takes place at 20-25% thickness strain range.

In the numerical simulation, neck initiation was plotted at nodes along the YSYMM axis for both models as a function of time to determine the relationship between thickness thinning and strain localization. As shown in Fig. 6 and 7, the deformation was initially uniform. Afterwards, the first neck initiated at about 25% tensile strain. According to the experimental results (Ref 12), the load reached the maximum when the tensile strain was about 20–25%. Both the results clearly showed that a considerable amount of extension took place after the diffuse necking. Visually, localized necking may be seen much later than diffuse necking occurs. In this study, it was observed that the visible necking usually took place at a thickness strain of about 20–25%. Therefore, it is proposed that the fracture criteria constants should be calculated at a thickness strain of about 20–25%, and are considered as critical values of the ductile fracture criteria for localized necking determination. The fracture criteria constants were calculated from the tensile

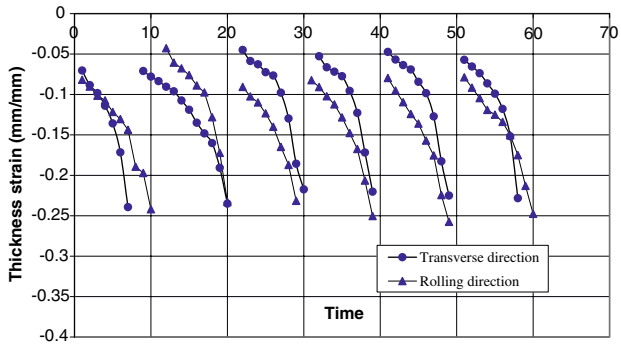

Fig. 5 Thickness strain from diffuse necking through fracture

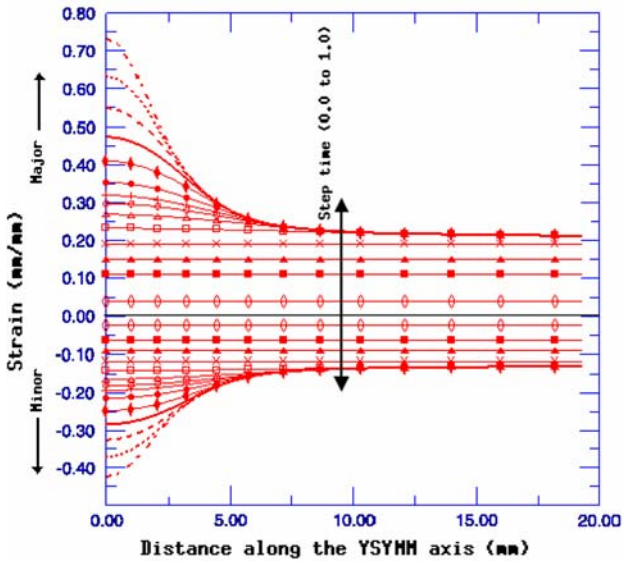

Fig. 6 Simulation of necking based on tensile test simulation (Hill's model)

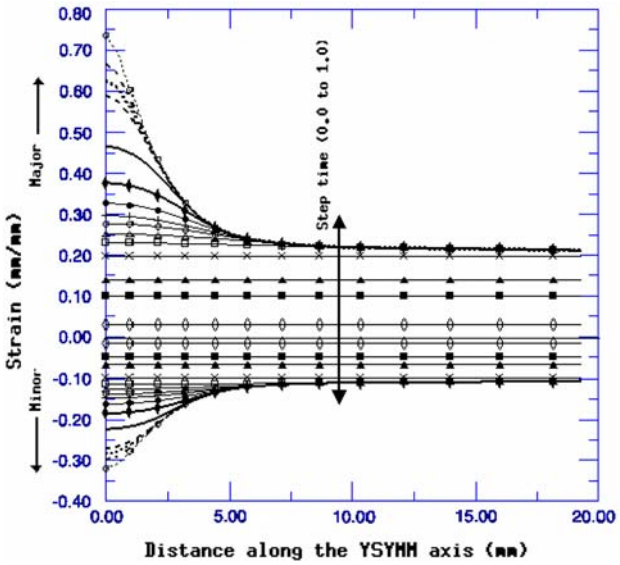

Fig. 7 Simulation of necking based on tensile test simulation (Mises' model)

Table 3 The summary of ductile fracture criteria constants at 20% and 25% thickness strains

	Hill's, 20%	Hill's, 25%	Mises', 20%	Mises', 25%
The Generalized Plastic Work	174	225	126	162
Cockcroft and Latham	176	229	127	164
Brozzo et al.	0.249	0.303	0.192	0.235
Oh et al.	0.505	0.622	0.388	0.477
Norris et al.	0.409	0.493	0.320	0.388
Atkins	0.286	0.345	0.241	0.292

test simulation data for 20 and 25% thickness strain. These results are summarized in Table 3.

The limit strains for the FLD were determined by substituting the values of stress and strain histories calculated by finite element simulation of the out-of-plane formability test to ductile fracture criteria. The ductile fracture criteria were tested with the constants in Table 3.

The FLDs were computed based on the new proposed method for an application of ductile criteria for the FLD predictions as shown in Fig. 8. Figure 8 indicates that the prediction of the left side of the FLD using new method is quite reasonable for the generalized plastic work (Ref 5), Cockcroft and Latham (Ref 6), and Oh et al. (Ref 9). For a general acceptance, this newly proposed methodology should be tested on several materials. Other criteria were also acceptable for some strain paths, but not the full negative strain side of the FLD. This study was also performed at the 25% thickness strain as shown in Fig. 9. The results of 25% thickness strain method show that predictions are close to the plane strain side is higher than the experimental and analytical FLDs. These results are still considered as reasonable. The experimental FLD close to the plane strain condition might not be accurate because there was not enough experimental data available to obtain accurate curve fitting in the region of plane strain. The right side of the FLD was not predicted successfully using this model.

The new method for necking prediction was also tested for the Mises model at the 20 and 25% thickness strain for the both

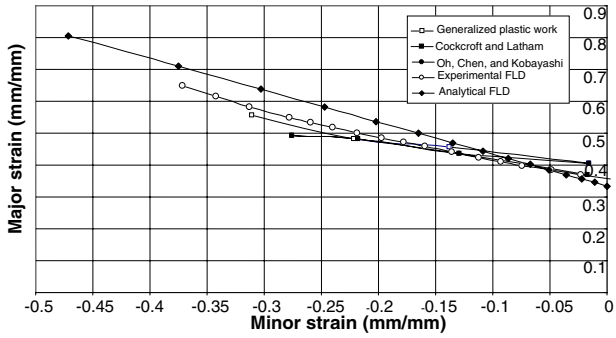

Fig. 8 Determinations of the left side of the FLD based on new methodology at 20% thickness strain (Hill's model)

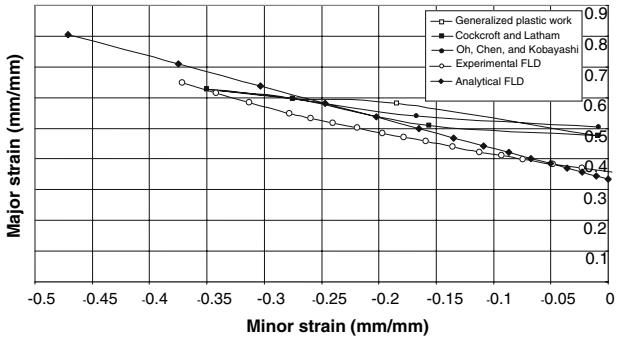

Fig. 9 Determinations of the left side of the FLD based on new methodology at 25% thickness strain (Hill's model)

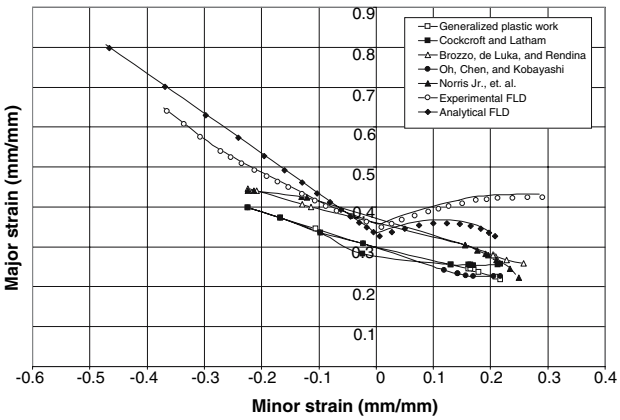

Fig. 10 Determinations of the FLD based on new methodology at 20% thickness strain (Mises' model)

side of the FLD. The results are shown in Fig. 10 and 11. New method at 20% thickness strain using the Mises Model, Brozzo et al. (Ref 8) and Norris et al. (Ref 10) criteria yielded an acceptable prediction at the left side of the FLD. However, predictions at the right side were not good, especially the prediction close to biaxial tension. Besides, they had better prediction than the generalized plastic work (Ref 5), Cockcroft and Latham (Ref 6) and Oh et al. (Ref 9) criteria. The predictions at 25% thickness strain revealed that the predictions at the left side of the FLD looked reasonable for each criterion

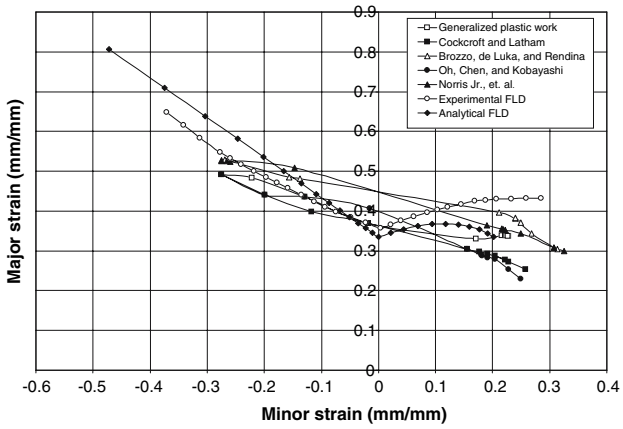

Fig. 11 Determinations of the FLD based on new methodology at 25% thickness strain (Mises' model)

(Fig. 11). At the right side of the FLD, the predictions by Brozzo et al. (Ref 8) and Norris et al. (Ref 10) had some improvement, but still underestimated the FLD. Other criteria had still much lower predictions than the experimental and analytical FLDs.

It is reasonable to expect to see some deviation from the experimental and analytical values predicted by the Mises model since an isotropy assumption employed in all calculations and simulations. The predictions based on the Mises model may not be compared with the experimental and analytical FLDs quantitatively. However, it is useful to see the effect of metal plasticity models.

5. Conclusion

Neck initiation prediction was used to determine the FLD by substituting the stress and strain histories calculated by the finite element simulation into the ductile fracture criteria. The ductile fracture criteria constants were calculated with the newly proposed method, in which fracture criteria constants were calculated at a thickness strain of about 20–25%, and be considered as a critical value for neck initiation. The left side of the FLD was predicted by the newly proposed methodology using both models and the predictions were quite successful. The use of the Mises model seemed to improve predictions for the right side of the FLD. For general acceptance, this new proposed methodology should be tested on several metals especially the metals with low ductilities.

Acknowledgment

The authors would like to thank Prof. C. R. Picu of Rensselaer Polytechnic Institute, Troy, NY for the fruitfull discussions.

References

1. S.E. Clift, P. Hartley, C.E.N. Sturgess, and G.W. Rowe, Fracture Prediction in Plastic deformation Processes, *Int. J. Mech. Sci.*, 1990, **32**, p 1–17
2. H. Takuda, K. Mori, H. Fujimoto, and N. Hatta, Prediction of Forming Limit in Deep Drawing of Fe/Al Laminated Composite Sheets Using Ductile Fracture Criterion, *J. Mater. Process. Technol.*, 1996, **60**, p 291–296
3. H. Takuda, K. Mori, and N. Hatta, The Application of Some Criteria for Ductile Fracture to the Prediction of the Forming Limit of Sheet Metals, *J. Mater. Process. Technol.*, 1999, **95**, p 116–121
4. H. Takuda, K. Mori, N. Takakura, and K. Yamaguchi, Finite Element Analysis of Limit Strains in Biaxial Stretching of Sheet Metals Allowing for Ductile Fracture, *Int. J. Mech. Sci.*, 2000, **42**, p 785–798
5. A.M. Freudenthal, *The Inelastic Behavior of Engineering Materials and Structures*, John Wiley & Sons, NY, 1950
6. M.G. Cockcroft and D.J. Latham, Ductility and the Workability of Metals, *J. Inst. Met.*, 1968, **96**, p 33–39
7. P.W. Bridgman, *Studies in Large Plastic Flow and Fracture*, McGraw-Hill, NY, 1952
8. P. Brozzo, B. Deluka, and R. Rendina, A new method for the prediction of formability in metal sheets. In: Proceedings of the Seventh Biennial Conference on Sheet Metal Forming and Formability, International Deep Drawing Research Group, 1972
9. S.I. Oh, C.C. Chen, and S. Kobayashi, Ductile Fracture in Axisymmetric Extrusion and Drawing, *J. Eng. Ind. Trans. ASME*, 1979, **101**, p 36–44
10. D.M. Norris Jr., J.E. Reaugh, B. Moran, and D.F. Quinones, A Plastic-Strain, Mean-Stress Criterion for Ductile Fracture, *J. Eng. Mater. Technol. Trans. ASME*, 1978, **100**, p 279–286
11. A.G. Atkins, Possible Explanation for Unexpected Departures in Hydrostatic Tension-Fracture Strain Relations, *Met. Sci.*, 1981, **15**, p 81–83
12. F. Ozturk and D. Lee, Analysis of Forming Limits Using Ductile Fracture Criteria, *J. Mater. Process. Technol.*, 2004, **147**, p 397–404
13. Hibbitt, Karlsson, and Sorensen, Inc., ABAQUS/Standard User's Manual II
14. W.F. Hosford and R.M. Caddell, *Metal Forming Mechanics and Metallurgy*, Prentice-Hall, Englewood Cliffs, NJ, 1993
15. A. Graf and W.F. Hosford, Calculations of Forming Limit Diagrams, *Metal. Trans. A*, 1990, **21**, p 87–93
16. F. Ozturk, Analysis of forming limits using ductile fracture criteria, Ph.D Thesis, Rensselaer Polytechnic Institute, Troy, NY, 2002
17. R. Hill, On Discontinuous Plastic States, with Special Reference to Localized Necking in Thin Sheets, *J. Mech. Phys. Solids*, 1952, **1**, p 19–30
18. H.W. Swift, Plastic Instability Under Plane Stress, *J. Mech. Phys. Solids*, 1952, **1**, p 1–18
19. S.P. Keeler and W.G. Brazier, Relationship between laboratory material characterization and press shop formability, *Microalloying 75 Proceedings*, Union Carbide Corp., NY, 1977, p 517–528